The temporal-spatial-fractal characters on Nino3.4 SST

Zhiyong HUANG and Hiroshi MORIMOTO

Department of Earth and Environmental Sciences
Graduate School of Environmental Studies
Nagoya University

Abstract.

There are many theories explaining the mechanisms of El Nino-Southern Oscillation (ENSO) evolution. For the purpose of better understanding the mechanisms of ENSO events, we propose the postulation of fractal analyzing self-organized criticality (fSOC) for ENSO cycle, on which critical condition of SOC is taken by the scaling behavior. A scaling behavior process has the property that the plots of logarithm of energy spectrum (signal's octave) against the logarithm of the timescale (frequency) nearly showed a straight line, called log-log plots. Discrete wavelet fractal estimator is applied to analyze temporal-spatial-fractal characters of sea surface temperatures (SSTs) over Nino3.4 area. The trends of Hurst parameter H anomaly well meet the oscillating characters of the intensity of ENSO event (ENSO-event-index). H can be an alternate ENSO index. A tail at the top of the log-log plots represents the strength of signal's octave at the largest timescale. The changes of the height of tail indicate the evolution of ENSO cycle. El Nino causes the tail to go up, La Nina causes the tail to go down, the threshold from warm to clod states is shown by an avalanche of the straight tail at the log-log plots. The key process that governs the ENSO process is the oscillation of timescale of 2^{10} days, (34 months). A timescale of about 68 months is found to be an important climatic measurement. In this study, we consider that the El Nino event starts from the Eastern Equatorial Pacific.

1 Introduction.

The El Nino-Southern Oscillation (ENSO) has been wildly researched for 60 years. There are many qualitative theories about the mechanisms responsible for ENSO, such as the delayed oscillator theory of ENSO, e.g. Suarez et al., [1], Battisti et al., [2], also [3], [4], [5]; and the chain of short sighted oscillators theory, e.g. J.S. Andrade Jr. et al., [6], etc.; There are two main modes on ENSO [3], that are Kelvin-like mode, e.g. Philander et al., [7], Yamagata, [8], etc.; and Rossby-like mode, e.g. Gill, [9], Hirst, [10], etc.. Based on the various theories of ENSO mechanisms, many forecasting models [11] have been developed for predicting ENSO phenomenon. A list of references of models can be found in Cecile Penland, [12], Barnett et al., [13], and M. Ausloos et al., [14]. They help to understand the physical processes of ENSO.

However, we cannot yet understand the mechanisms responsible for ENSO perfectly, T.P. Barnett et al., [13]. It is important to understand the boundary conditions of evolution of ENSO cycle. The boundary conditions are: (1) the condition of warming, which starts the El Nino phenomenon, and (2) the condition of cooling, which ends warming and starts the La Nina phenomenon, Michael J. et al., [15]. It is also fundamental to understand the key process of ENSO, which usually refers to the magnitude and timing of predicted ocean surface temperatures, especially on the low frequency, large-scale changes [16].

The aim of this paper is to address the problems mentioned above, and might help improving the predictability of ENSO event, but does not aim to develop any realistic model of ENSO. The fractal analysis based on the concept of Self-Organized Criticality (SOC) is an alternate tool for the purpose. We name the method of fractal analysis based on the concept of SOC as fractal analyzing SOC (fSOC for the short).

Fractal character is also similarly called scaling behavior, or scaling, long-time memory, and $1/f$ spectra or Flicher noise.

Scaling means invariance properties of the time series aggregated (or averaged) on different timescales, defined by Demetris Koutsoyiannis, [17]. The property of scaling is similar to the Gutenberg-Richter law [18]. That is, the logarithm of the frequency of events decreases linearly with their

magnitude [19].

Therefore, a long-time memory process has a power law spectrum distribution that plots as a straight line on the logarithm of energy spectrum (signal's octave) against the logarithm of the timescale (roughly said frequency). We will call the log-log plotted energy spectrum, log-log plots.

However, there is a tail at the top of log-log plots that represents the energy spectrum (signal's octave) at the largest scale [20], because in the physical world, the time series of temporal or spatial scales are finite, it limits the signal's octaves or averaged energy spectrum at the largest scale. Therefore the changes of the height of the tails correspond to the random variant of energy spectrum at the largest scale.

Self-Organized Criticality is one of the four main theoretical explanations for the $1/f$ spectra [21], see [22] for a review Klaus Fraedrich et al., [23]. A specific description of the concept of the SOC can be found in J.S. Andrade Jr. et al., [6]. Originally, it was proposed by Bak, Tang, and Wiesenfelf (BTW), [24], on which they used a sand pile model to explain a cellular automata model. After that it was taken as a way to explain phenomena as diverse as earthquakes, the stock market, forest fires, quaternary ice volume fluctuations, magnetosphere, and ecology. Some experiments and many simulations have been conducted.

What is in fact fSOC? In a word, it means that the critical condition of SOC is taken by the scaling state. It implies three facts: First, the log-log plots have a straight tail. Second, the straight tail of log-log plots implies that the corresponding timescale takes a high energy spectrum. Third, a high energy spectrum of the process stays at the critical state that will result in an avalanche at the corresponding timescale.

ENSO cycle can be described by the concept of fSOC associated with the changes of tails of log-log plots. El Nino events indicate the low frequency and large-scale changes in the tropical ocean-atmosphere system, T.Barnett et al., [16]. Before the El Nino event, a long-term, large-scale warming process of sea surface temperature (SST)over the tropical Pacific happens. The warming process of SST enhances the amplitude of the energy spectrum at large scale. It reflects a raising tail process at log-log plots at the large scale. When the warming of SST is continuous, El Nino happens. The energy spectrums reach the critical state. It appears as a

straight tail of the log-log plots. Based on concept of fSOC, the critical state will result in an avalanche of energy spectrum at large-scale with the tail falling down. It reflects the ocean's release of energy at large scale. At the same time, it becomes the threshold from warm to clod states.

To demonstrate the postulation of fSOC for ENSO, a spatial-temporal-spectral analysis is carried out. A.L. Wang, et al., [25], and E.J., McCoy et al., [26], have shown that the Wavelet Transformed Method had the advantage of spectrum analysis for estimated Hurst parameter H. Here, we analyze the temporal and spatial fractal characters on SSTs over Nino3.4. Discrete wavelet spectral estimator, Rene Carmona et al., [20], is applied in this study. The Wavelet Explorer version 1.2 for Mathematica5.1 is employed. Daubechies Filter with order2 is carefully selected for the procedure, since the skew character of Daubechies order2 wavelet is the best wavelet to meet the asymmetric nature ([5],[12], [27], [28], [29]) of the warm and cold phases of SST. Periodic boundary of Wavelet Transform is applied in this study. For catching the period of ENSO cycle, a shifting time window of $D = 2^{11}$ days (68 months), is applied for the Discrete Wavelet Transform (DWT).

From the analysis of SST fluctuations over Nino3.4, we obtain the following results: The trends of H anomaly well meet the oscillated characters of ENSO-event-index (Fig. 2). H can be an alternate ENSO index. It might help improving the predictability of ENSO. The initiating condition of El Nino is described here as a raising tail process, which is associated with the changes of energy spectrum at a 2^{10}-day timescale (34 months) (Fig. 1). When the El Nino event reaches its maximum amplitude, the tail reaches the straight state along the line of log-log plots. The extreme conditions or unusually rapid transitions between warm and cold conditions are considered as an avalanche of the tail. The results that are shown in Fig. 1 nearly agree with the postulation of fSOC for ENSO. The key process that governs the ENSO cycle is mainly due to the changes of signal's octave at a 2^{10}-day timescale (34 months). The El Nino event starts from the Eastern Equatorial Pacific in the Nino3.4, which is mainly affected by Rossby waves. A 2^{11}-day timescale (68 months) is an important climatic measurement, since a shifting time window of 2^{11} days (68 months) can catch the spectral natures of ENSO more comprehensively.

2 On the data sets.

2.1 On the SST data sets, and Nino3.4 SST index.

The SST data sets used here is obtained from TAO (the Tropical Atmosphere Ocean Project) [30], daily from July 21^{st}, 1991 to October 31^{st}, 2005, composed of 20 stations, positioned at the crossed points of longitude 5^oN, 2^oN, 0^o, 2^oS, 5^oS and latitude 170^oW, 155^oW, 140^oW, 125^oW over Nino3.4, [31].

The Nino3.4 SST index is a measurement of the El Nino (or oceanic) component of ENSO, and is one of the main indices of the ENSO event (NOAA), consisting of the area-averaged SST over Nino3.4.

We group every five banded stations, which are lined along longitude from 5^oN, 2^oN, 0^o, 2^oS, to 5^oS, and call those groups 'site'.

Therefore, there are 4 sites in Nino3.4, namely, the sites at $170W^o$, 155^oW, 140^oW and 125^oW, lined along the Eastern Equatorial Pacific.

2.2 The procedure of data correcting.

The numbers of missed records at 4 equatorial stations from July 21^{st}, 1991 to October 31^{st}, 2005, are 41, 30, 190, and 636 for stations 0^oN 170^oW, 0^oN 155^oW, 0^oN 140^oW, and 0^oN 125^oW, respectively. The effects of missed records are trivial, except for the station of 0^oN 125^oW.

In order to correct the missed records at the stations, we simply insert the mean of the whole SST time series of a station to the missed record.

To generate Nino3.4 SST index, an area-averaged SST over Nino3.4 is evaluated. We perform the following three steps: First, the SST of a site, which consists of five stations, is calculated by averaging the five corresponding records. The missed records are filled by 0.0. The data gaps are not accounted into the statistical number (e.g., mean of $\{12, 14, gap, 15, gap\}$ =mean of $\{12, 14, 15\}$). Some data gaps remain. The numbers of remained data gaps at four sites are: 6 for 170^oW, 0 for 155^oW, 0 for 140^oW, and 105 for125^oW. Second, Nino3.4 SST index is calculated by averaging the four corresponding sites of SST. The data gaps are evaluated as 0.0 during site-averaged process. The data gaps are not accounted into the statistical number, either. A few data gaps remain. Third, a few remained data gaps

are simply filled by the mean of the whole time series. So far, Nino3.4 SST index is generated.

2.3 On the ENSO-event-index.

In this study, ENSO-event-index is the numerical value given to the intensity of ENSO-event in a given year, which equals to one of the following seven values: -1.5 (strong La Nina), -1 (moderate La Nina), -0.5 (week La Nina), 0 (neutral year), 0.5 (week El Nino), 1 (moderate strength El Nino), and 1.5 (strong El Nino), [32], [33].

The years of ENSO-event-index are shown as following:

{1991, 1.0}, {1992, 0.5}, {1993, 0.5}, {1994, 1.0}, {1995, -0.5}, {1996, 0.0}, {1997, 1.5}, {1998, -1.0}, {1999, -1.0}, {2000, -0.5}, {2001, 0.0}, {2002, 1.0}.

3 Methods.

3.1 The definitions of fractional Brownian motion and Hurst parameter.

Definition: fractional Brownian motion (fBm for short), followed by Rene Carmona et al., [20].

A fractional Brownian motion is a mean zero (non-stationary) real Gaussian process $f(x) \in R$ with stationary increments, and an autocovariance function satisfied

$$E\{f(x)f(y)\} = \frac{\sigma^2}{2}\{|x|^{2H} + |y|^{2H} - |x-y|^{2H}\}, \quad (3.1)$$

where $\sigma > 0$ and $0 \leq H \leq 1$.

The H is called the Hurst exponent of the process, or called Hurst coefficient, Hurst parameter.

When $H = 1/2$, the definition (3.1) gives

$$E\{f(x)f(y)\} = \sigma^2 min\{x, y\}, \quad (3.2)$$

which shows the classical Brownian motion.

3.2 The Wavelet-based method is a good tool for estimating H.

There are many methods for estimating the Hurst parameter, such as the Box Counting method, the Yardstick method, the Co-variation method, the Structure Function method, the Variation method, the Power Spectrum method, and the Rescaled rang analysis (R/S analysis) method, etc., see A.L. Wang et al., [25], for a review. The power spectrum analysis methods include the Fourier-based method and wavelet-based method.

Wavelet-based method has been demonstrated as a good tool for estimating Hurst coefficient. A.L. Wang et al., [25] have done a comparing work, and showed that the Wavelet Transform method could accurately calculate Hurst parameter. E.J. McCoy et al., [26], also showed that Wavelet-based method was better than Fourier-based method, and showed that Wavelet-based method was a good tool for estimating the Hurst parameter.

3.3 Discrete Wavelet spectral estimators for Hurst parameter H.

Here, the discrete type of the Wavelet Spectral Estimator is employed. More detail on continuous type of the Wavelet Spectral Estimator, please refer to Rene Carmona et al., [20], page 254-page 258.

3.3.1 The wavelets.

A fixed function $\psi(.) \in L^1(R) \cap L^2(R)$, is called mother wavelet of the analysis.

$\psi_{b,a}$ is called wavelet, defined as follow

$$\psi_{b,a}(x) = \frac{1}{\sqrt{a}}\psi(\frac{x-b}{a}), \tag{3.3}$$

$x \in R$, $b \in R$, and $a \in R_+^*$.

Remark [20]:

When studying fractional Brownian motions, we use the normalized wavelets (3.3), rather than the definition of

$$\psi_{b,a}(x) = \frac{1}{a}\psi(\frac{x-b}{a}). \tag{3.4}$$

3.3.2 On the Discrete Wavelet spectral estimator for H.

The discrete wavelet, $\psi_{j,k}(t)$ has the form

$$\psi_{j,k}(x) = 2^{j/2} \cdot \psi(2^j x - k), \tag{3.5}$$

where $x \in R$, and $j, k \in Z$.

The discrete wavelet transforms (DWT), $d_{j,k}(x)$ of a finite-energy signal f is defined as follow

$$\begin{aligned} d_{j,k}(x) &= \int f(x)\psi_{j,k}(x)dx \\ &= \int f(x) \cdot 2^{j/2} \cdot \psi(2^j x - k)dx. \end{aligned} \tag{3.6}$$

The value of $d_{j,k}(x)$ contains the information concerning the signal f at the scale $a = 2^{-j}$ around point $b = 2^j k$.

Formula 1:

Under some mild assumptions on the mother wavelets, the DWT of a fBm with Hurst coefficient H satisfies

$$E\{d_{j,k}(x)d_{j_1,k_1}(x)\} = -2^{(j+j_1)/2}\frac{\sigma^2}{2}\int\int |x-y|^{2h}\psi(2^j x - k)\psi(2^{j_1} y - k_1)dxdy. \tag{3.7}$$

Formula 2: Discrete wavelet spectral estimator $V_b(a)$:

$$V_b(a) = E\{d_{j,k}^2(x)\} = C_2 \cdot 2^{-(2H-1)j}, \tag{3.8}$$

where $d_{j,k}^2(x)$ can be roughly viewed as the averaged energy over scale $a = 2^{-j}$.

A linear fitted on

$$log_2 E\{d_{j,k}^2(x)\} = -(2H+1)j + log_2(C_2), \tag{3.9}$$

yields the slope of fitted line, namely $slope = -(2H+1)$.

Therefore, the discrete wavelet spectral estimator for H has the form

$$H = \frac{-slope - 1}{2}. \tag{3.10}$$

3.4 Procedure of calculation.

The Wavelet Explorer version 1.2 for Mathematica5.1 is employed. DWT with DaubechiesFilter(2) is carefully selected, since the skew characters

of Daubechies order2 wavelet is the best wavelet to meet the asymmetric nature [12] [27] [28] of the warm and cold phases of SST, or the asymmetry of El Nino-La Nina events [29], or the ENSO asymmetry cycle mode that was designed by Nagai et al., [5]. Periodic boundary of wavelet transform is applied for the study. A shifting time window of $D = 2^{11}$ days (68 months) is the best length for analysis.

To investigate the temporal-spatial-fractal characters over Nino3.4 SST, we do the following three steps:

First, we investigate the changes of energy spectrum on Nino3.4 SST time series at the different scales, and the oscillations of tails of log-log plots. We shift the time window of $D = 2^{11}$ days (68 months), by changing the initial point of D. The initial point of D is set on January 1^{st} of each year, except for 1991, which starts from July 21^{st}. There is a total of 10 panels of log-log plots shown on Fig. 1. Therefore, there are 10 different values of H.

Second, we compare the trend of H oscillation on Nino3.4 SST with the trend of ENSO-event-index intensity. Those are shown in Fig. 2. Also, the trends of H at the other three stations are attached for contrasting.

Finally, to investigate the spatial fractal characters of Nino3.4 SST, we calculate the average of the 10 values of H at each station and at Nino3.4. The result of situations $D = 2^8, 2^9, 2^{10}, 2^{11}$ are all compared. As shown in Fig. 3.

4 Results and discussion.

4.1 El Nino causes an upwards tail, La Nina causes a downward tail, the threshold causes a straight tail at the log-log plots.

A nearly straight tail of log-log plots is clearly shown in the panels of 1991, 1994, 1997 (Fig. 1), in which El Nino happened strongly. The straight tail means that the energy spectrum scaled at the size of 2^{10} reaches its maximum amplitude, and the system will result in an energy avalanche (panels of 1995 and 1998). We believe that it may represent fSOC associated with El Nino. When the tail rises, it implies an El Nino formation process. When the tail falls down, La Nina occurs. The straight tail describes a threshold from El Nino phase to La Nina phase.

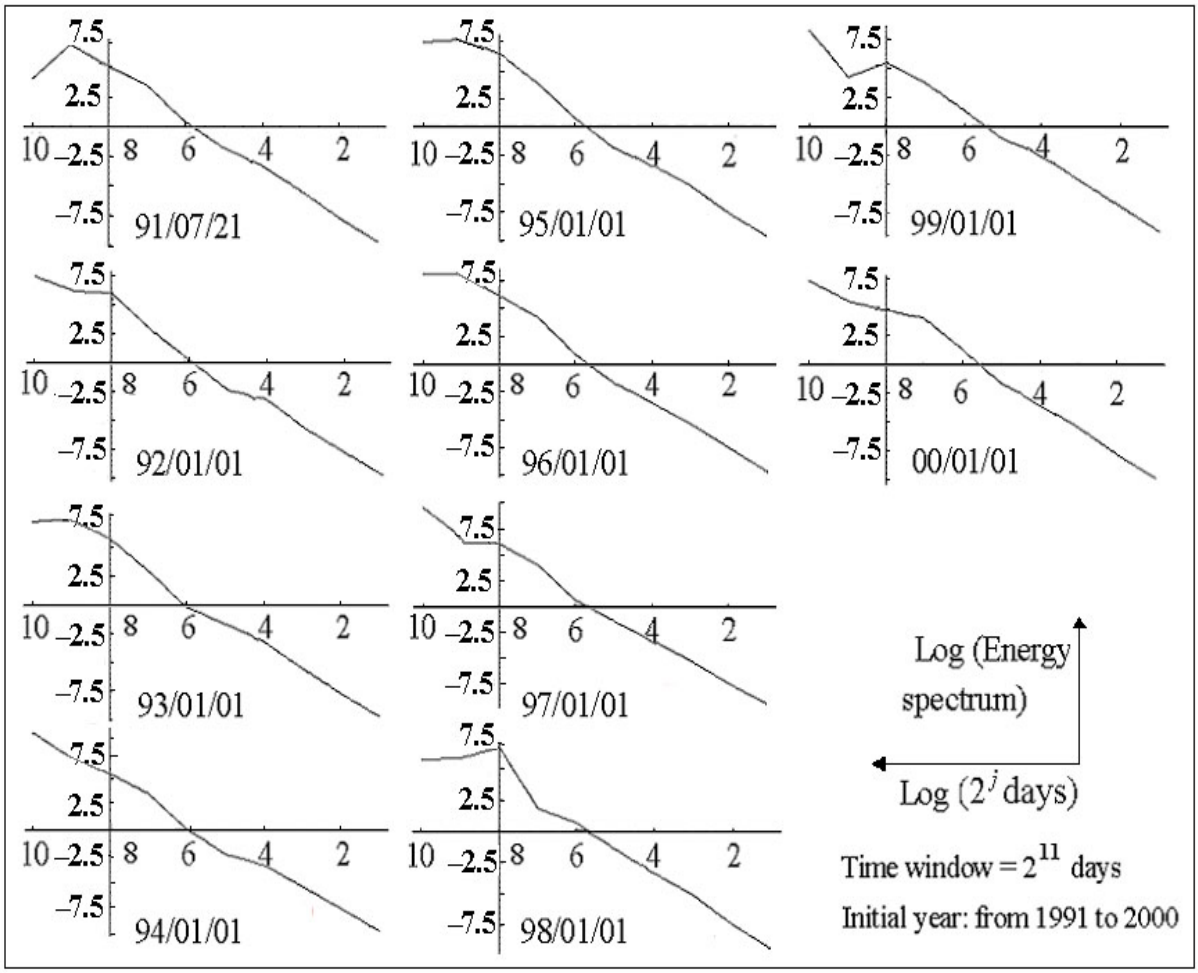

Figure 1: The log-log plots of the wavelet energy spectrums.

Fig. 1. Spectral analysis for Nino3.4 SST with time window of $D = 2^{11}$ days (68 months). There are 10 panels corresponding to the 10 different initial points of time window D, respectively. Initial points are January 1^{st} of 1992 to 2000, except the first panel, in which D starts from July 21^{st} 1991. Each panel shows the log-log plots of the logarithm of wavelet spectral estimator $V_b(a)$ against the logarithm of the timescale a. The horizontal axis represents the logarithmic timescale. The vertical axis is the logarithm of wavelet spectral estimator $V_b(a)$ or simply the energy spectrum.

The variant of tail implies the dynamics of oceanic heat storage. Since the changes of the tail height correspond to the changes of the signal's octave at the 34^{th} month of the timescale. It shows that the system is strongly affected by a long-time memorized oscillation in that point. The high frequencies of SST mainly come from atmospheric fluctuation, M.J.

McPhaden, et al., [15]. And low frequencies of SST are mainly attributed to the ocean energy oscillation, Klaus Fraedrich et al., [23]. 'Oceanic Long-time Memory', e.g. M.J. McPhaden et. al., [15], S. Levitus et. al., [34], is supported by the Delayed Oscillator Theory of ENSO, e.g. Suarez et al.,[1], Battisti et al., [2], etc. In this study also call long-time memory as low frequency, or large timescale. So the changes of large energy spectrums are mainly affected by the oceanic heat oscillations, normally referred as Kelvin-Rossby waves or Ekman current.

There are complex processes that cause a persistent warm SST in the Central Equatorial Pacific during El Nino. It is mainly due to Kelvin waves, Rossby waves, and Ekman current coupled geotropic current. It is said that El Nino mainly has two types, 1982-83 type due to Ekman current, T.P. Barrnett et al., [13], and 1972 type due to Kelvin-Rossby waves, Nagai, et al., [5]. Kelvin waves appear in the Pacific every winter, however, El Nino does not occur every year [35]. Only when those kinds of waves or currents carry sufficient energy reaching the Nino3.4 area, El Nino grows up, and the tail of log-log plots raises, and it will eventurally reach the straight line state of log-log plots, which means that the system reaches its critical state of maximum amplitude for El Nino, i.e. the Walker circulation breaks, and trade wind weakens. They represent an avalanche on climate system along the Equatorial Pacific with large releases of energy from the ocean. After a threshold from warm conditions to cold conditions, La Nina starts. The tail of log-log plots falls down.

The oscillation of the 2^{10}-day timescale is a key process which governs the ENSO cycle. El Nino is initiated from large scale.

It is worth to note that the relationship between the scaling behavior and the physical ocean dynamic process can be found in Klaus Fraedrich et al., [23]. That is a model-based research on scaling behavior (long-time memory) of the ocean. They concluded that scaling behavior beyond decades scale is a result of horizontal advection in the North Atlantic, and the low-frequency within scaling behavior 1-100 year in the South Pacific is caused by local vertical diffusion [23].

4.2 The value of H as an alternate ENSO index.

The trend of H anomaly nearly matches the trend of the curve of ENSO-event-index (Fig. 2). H can be an alternate ENSO index. We have discussed this in section 4.1. When the tail rises, it indicates El Nino formation process. When the tail falls down from the straight tail, it means a threshold from El Nino to La Nina. A higher tail results in a bigger slope of log-log plots. It causes a bigger value of H. So the values of H follow well the ENSO-event-index in its oscillatory behaviors.

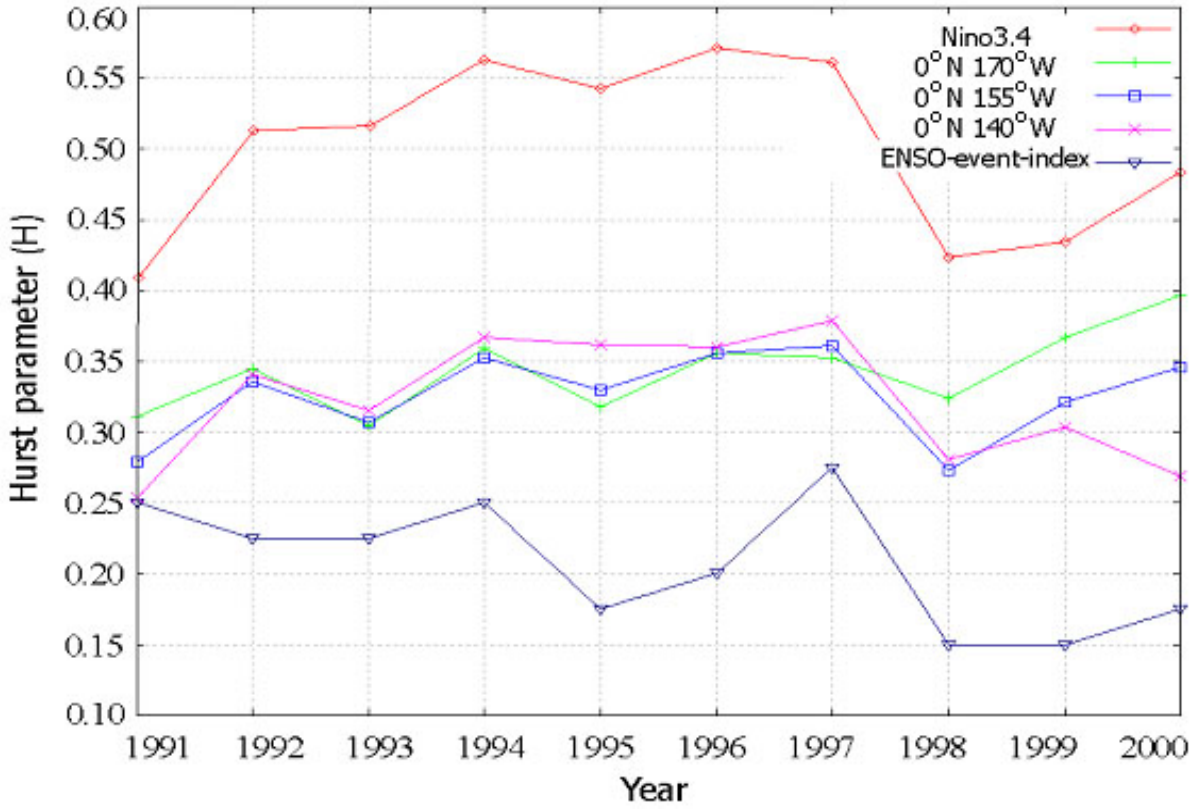

Figure 2: Trend of H and ENSO-event-index meet together

Fig. 2. The temporal and spatial patterns of H associated with ENSO-event-index. The horizontal axis is the initial year of time interval D. The vertical axis is the value of Hurst parameter. A time window of D=2^{11} days (68 months) is selected. The results of H at the stations of 0^{o}N 170^{o}W, 0^{o}N 155^{o}W, 0^{o}N 140^{o}W, and at the Nino3.4 are shown accordingly. An additional curve of ENSO-event-index is attached for comparison.

A time window of 2^{11} days (68 months) is the best interval for analysing

the ENSO cycle. DWT requires a timescale of 2^i days as the basic component for transformation. However, when the other time windows of say, 2^8 days, 2^9 days, and 2^{12} days are applied for the study, all of them can not show as good results as the applied time window of 2^{11} days do.

It is worth to note that there are other researchers who have reported that about 5.5 years is an important climatic measurement. M. Ausloos and K. Ivanova, [36], also Richard Metzler et al., [37], showed that there was a crossover at about 64 months on the scaling behavior when they analyzed the southern oscillation index (SOI) during 1866-2000. A. RuizdeElvira et al., [38], found that the 5 years timescale showed the maximum probability for climatic predictability, when they analysed the zonal wind over the tropical Indian and Pacific. Nagai et al., [5], used an ENSO cycle mode with a period of 5 years, which contained one warm process and two cold processes, to simulate SST anomaly and got fairly reasonable results.

This property was explained by Michaelsen [39] as a consequence of a positive feedback mechanism that could govern the processes of the atmosphere-ocean interaction in the regions of intensive cyclonic activity [40] (also see e.g. White, 1975, Nicholls, 1981, or V.E. Privalsky, 1987).

This result may extend the limits of statistical predictability to six years against 1 or 2 years in the scale case.

Fig. 2. also illustrates that the different stations have similar values of H around 0.34, except for the starting point of July 1991 and after 1999. It strongly indicates that the system is Self-Organized with respect to spatial pattern.

4.3 The El Nino event is initiated in the Eastern Equatorial Pacific

First, Fig. 3. represents decreasing values from station 0^oN170^oW to 0^oN140^oW, through 0^oN155^oW, except for $D = 2^8$. The trends may vary descreasing from 0.5 to 0 or ascend from 0.5 to 1. This demonstrates trends that depart from the non-memory state (Brownian motion). It describes that the lower the longitude the longer the memory of SSTs. So the changes of long memorized oscillation mainly come from low longitude locations.

On the other hand, since the El Nino is initiated from large scale on which we have discussed in section 4.1, it is reasonable to believe that the

long-time memory is carried by the large-scale. So far, we can declare that El Nino is initiated from long memorized oscillation that mainly comes from lower longitude locations in Nino3.4.

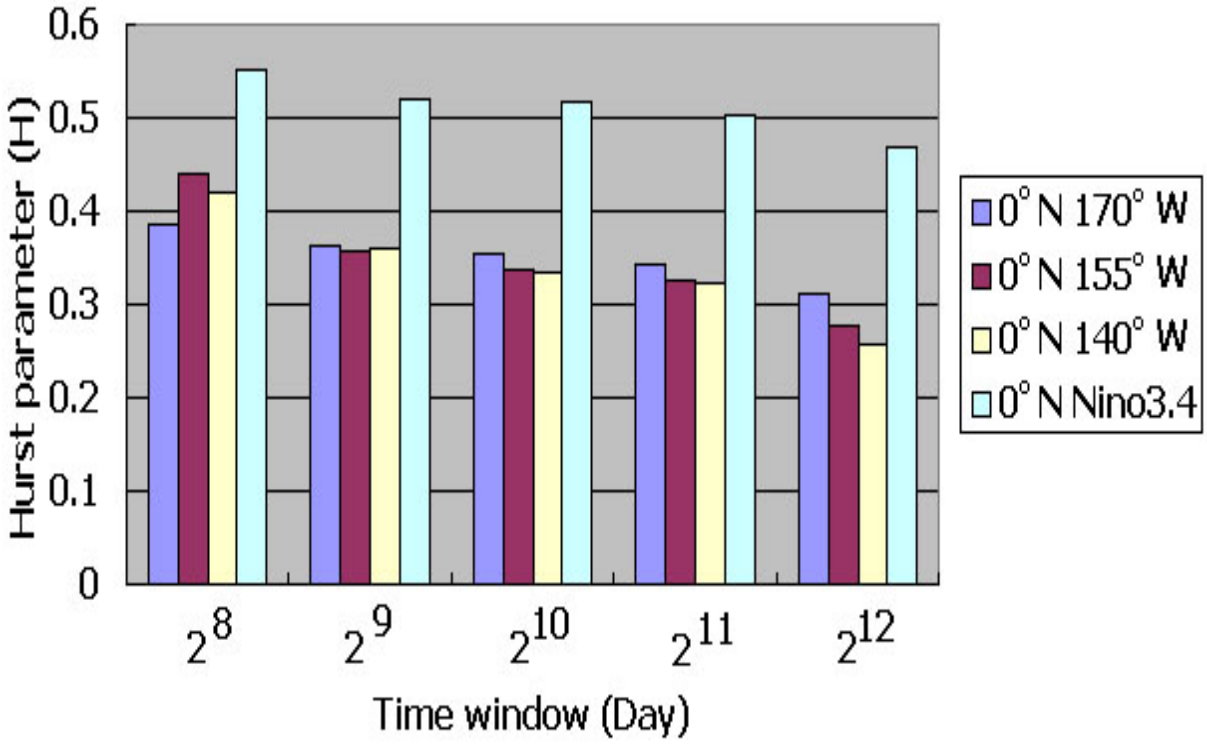

Figure 3: The temporal and spatial pattern of H

Fig. 3. The spatial characters of mean of H with respect to different time windows of D. The horizontal axis is a list of stations of 0^oN170^oW, 0^oN155^oW, 0^oN140^oW, and the Nino3.4. The vertical axis is the mean of H at each station. Four curves respond to four fixed time windows D, respectively. The curves represent the changes of mean of H with respect to the spatial pattern.

Therefore, El Nino is initiated from the Eastern Equatorial Pacific. This result matches the classical El Nino that initiates the air-sea interaction in the Eastern Equatorial Pacific. T. Tozuka et al., [42], also found the westward expansion of the SSTA (sea surface temperature anomaly) along the 5^oN line. It is similar to the direction characteristics of Rossby waves, e.g. Gill, [9], Hirst, [10], etc.. Actually, SST is defined as temperatures in the uppermost layer (2.8m) [5] where Rossby waves transport westward. However, the Kelvin waves, e.g. Philander et al., [7], Yamagata, [8], actively

transport eastward is a little deeper.

Second, Fig. 3. illusratess that there are significant different fractal characters between the local stations and the Nino3.4 region.

Nino3.4 SST itself is a Brownian motion because its H nearly equals 0.5. But for a station, the SST time series shows that it is not a Brownian motion, since it keeps a long memory with the H below 0.34. This means that the SST time series of a region may show a Brownian motion character, but the SST time series of a local point in the region, will not be a Brownian motion. It needs to be explained mathematically in the future.

The scaling behavior does not hold everywhere. The temporal and spatial fractal characters have been reported in many articles. Model-based researchers such as Demetris Koutsoyiannis, [17], K.M. van Vliet et al., [1], have demonstrated that the scaling behavior can be produced by a simple dynamic model associated with proper fractal noise. However, both data-based [41] and model-based [23] [41] researchers have showed that there was a little variant value of H around 0.5. Moreover, M. Ausloos et al., [14], agreed that scaling laws do not hold everywhere.

Third, Fig. 3. describes that the bigger time window of D, is the smaller H results. It indicates that the value of H is affected by the time window selected. The reason is the energy spectrum of a large timescale cannot be completely captured in a shorter time window, when a DWT is applied.

5 Conclusion.

In this paper, we have investigated several important issues on understanding the mechanisms of ENSO cycle, such as key process of ENSO cycle, boundary condition of initiating El Nino and threshold from El Nino to La Nina.

For the purpose of better understanding the mechanisms of ENSO, we propose the postulation of fSOC as follows. That is, according the hypothesis of Self-Organized Criticality, a signal has many time-scales. The signal's octave at any scale oscillates randomly. But it follows certain boundary conditions. The boundary condition is taken as the straight line of the log-log plots of energy spectrum of scaling behavior.

If we analyze a finite time series, investigating the log-log plots by shift-

ing the time window along the time series, the changes of signal's octaves or energy spectrum at large-scale are shown as an actively oscillation of tail at the top of the log-log plots.

The hypothesis of fSOC is applied to improve the understanding of the ENSO cycle. Only by using the DWT for temporal-spatial-fractal analysis, we find some very important fractal characters on ENSO attractor. The results are summarized as following:

The changes of fractal characters are affected by the ENSO development. ENSO development process is shown by the changes of fractal characters. The trends of H anomaly well meet the oscillated characters of ENSO-event-index. H can be an alternate ENSO index (Fig. 2).

The key process that governs the ENSO process is the oscillation of signal's octaves at large-scale of 2^{10} days (34 months). The height of the tail at the top of log-log plots indicates the strength of the signal's octave associated with timescale (frequency) of 2^{10} days. When the tail rises, it shows a warming process of SST, or El Nino formation. When the tail state is more horizontal, El Nino happens. When tail falls down, it is a threshold from El Nino to La Nina (Fig. 1).

El Nino is initiated from the Eastern Equatorial Pacific in Nino3.4, that is probably due to Rossby waves (Fig. 3).

A 2^{11}-day timescale (68 months) is found to be an important climatic measurement (Fig. 2).

It is important to extensively analyze the SSTs in the future.

6 References.

[1]. Suarez M.J., and P.S. Schopf, A delayed action oscillator for ENSO, Journal of the Atmospheric Science, Vol. 45, (1988), 3283-3287.

[2]. Battisti, D.S., and A.C. Hirst, Interannual variability in the tropical atmosphere-ocean system: Influence of the basic state, ocean geometry, and nonlinearity, Journal of the Atmospheric Science, Vol. 46, (1989), 1687-1712.

[3]. The Physics of ENSO, U.S. National Report to IUGG, 1991-1994, Reviews of Geophysic. Vol. 33 Suppl., 1995 American Geophysical Union,

http://www.agu.org/revgeophys/battis01/node3.html

[4]. S.G. Philander, El Nino and La Nina predictable climate fluctuations, Reports on Progress in Physics, Vol. 62, (1999), 123-142.

[5]. T. Nagai, T. Tokioka, M. Endoh, and Y. Kitamura, El Nino-Southern Oscillation simulated in an MRI Atmosphere-Ocean Coupled General Circulation model, Journal of Climate, Vol. 5, (1992), 1202-1233.

[6]. J.S. Andrade Jr., I. Wainer, J. Mendes Filho, and J.E. Moreira. 1994, Self-organized criticality in the El Nino Southern Oscillation. Physica A, Vol. 215, (1995), 331-338.

[7]. Philander, S.G.H., T.Yamagata, and R.C. Pacanowski, Unstable air-sea interactions in the tropics, Journal of the Atmospheric Science, Vol. 41, (1984), 604-613.

[8]. Yamagata, T., Stability of a simple air-sea coupled model in the tropics, in Coupled Ocean-Atmosphere Models, edited by J.C.J. Nihoul, pp. 637-657, Elsevier Oceanography Series, No. 40, Elsevier, Amsterdam, (1985).

[9]. Gill, A.E., Elements of coupled ocean-atmosphere models for the tropics, Coupled Ocean-Atmosphere Models, edited by J.C.J. Nihoul, Elsevier Oceanogr. Ser., 40, Amsterdam, (1985), 303-327, .

[10]. Hirst, A.C., Unstable and damped equatorial modes in simple coupled ocean-atmosphere models, Journal of the Atmospheric Science, Vol. 43, (1986), 606-630.

[11]. http://www.cpc.ncep.noaa.gov products/analysis-monitoring/ bulletin/forecast.shtml

[12]. Cecile Penland, A stochastic model of IndoPacific sea surface temperature anomalies, Physica D, Vol. 98, (1996), 534-558.

[13]. T.P. Barnett, M. Latif, E. Kirk and E. Roeckner, On ENSO Physics, Journal of Climate, Vol. 4, (May, 1991), 487-515.

[14]. M. Ausloos and K. Ivanova, Reply to " Comment on ' Power-law correlations in the southern-oscillation-index fluctuations characterizing El Nino' ", Physical Review E, Vol. 67, (2003), 068201.

[15]. Michael J. McPhaden, Thierry Delcroix, Kimio Hanawa, Yoshifumi Kuroda, Gary Meyers, Joel Picaut, and Mark Swenson, The El Nino-Southern Oscillation (ENSO) Observing System, Observing the Ocean in the 21st Century, C.J. Koblinsky and N.R. Smith (Eds), GODAE Project

Office and Bureau of Meteorology, Melbourne.

[16]. T. Barnett, N. Graham, M. Cane; S. Zebiak, S. Dolan; J. O'Brien, D. Legler, On the Prediction of the El Nino of 1986-1987, Science, Vol. 241, No. 4862, (Jul. 8, 1988), 192-196.

[17]. Demetris Koutsoyiannis, A toy model of climatic variability with scaling behaviour, Journal of Hydrology, Vol. 322, (2006), 25-48.

[18]. B. Gutenberg and C.F. Richter, Magnitude and energy of earthquakes, Ann. Geofis. (Rome), Vol. 9, (1956), 1-15.

[19]. J.M. Carlson and J.S. Langer, Mechanical model of an earthquake fault, Physical Review A, Vol. 40, Number 11, (December 1, 1989), 6470-6484.

[20]. Reni Carmona, Wen-Liang hwang, and Bruno Torresani, Practical Time-Frequency Analysis, Gabor and Wavelet Transforms with an Implementation in S. In 'Wavelet Analysis and Its Applications, Vol. 9, Charles k. Chui, Series Editor'. Academic Press, (1998).

[21]. S. Maslov, C. Tang, and Y.-C. Zhang, 1/f noise in Bak-Tang-Wiesenfeld models on narrow stripes, Physical Review Letters. Vol. 83, (1999), 2449.

[22]. M. B. Weissman, 1/f noise and other slow, nonexponential kinetics in condensed matter, Reviews of Modern Physics, Vol. 60, (1988), 537 .

[23]. Klaus Fraedrich, Ute Luksch, and Richard Blender, 1/f model for long-time memory of the ocean surface temperature, Physical Review E, Vol. 70, (2004), 037301.

[24]. Per Bak, Chao Tang, and Kurt Wiesenfeld, Self-Organized Criticality: An explanation of 1/f Noise, Physical Review Letters, Vol. 59, (27 July 1987), 380-384.

[25]. A.L. Wang, C.X. Yang, X.G. Yuan, Evaluation of the wavelet transform method for machined surface topography1: methodology validation. Tribology International, Vol. 36, (2003), 517-526.

[26]. E.J. McCoy and A.T. Walden, Journal of computational and Graphical statistics, Vol. 5, Number 1, (1996), 26-56.

[27]. Adam Hugh Monahan, and Aiguo Dai, The Spatial and Temporal Structure of ENSO Nonlinearity, Journal of Climate, Vol. 17, (2004), 3026-3037.

[28]. Hannachi, A. D. Stephenson, and K. Sperber, Probability-based

methods for quantifying nonlinearity in the ENSO. Climate Dynamics, Vol. 20, (2003), 241-256.

[29]. Monahan, A.H., Nonlinear principal component analysis: Tropical Indo-Pacific sea surface temperature and sea level pressure. Journal of Climate, Vol. 14, (2001), 219-233.

–, A simple model for the skewness of global sea surface winds. Journal of the Atmospheric Science, Vol. 61, (2004), 2037-2049.

[30]. http://www.pmel.noaa.gov/tao/index.shtml.

[31]. http://www.pmel.noaa.gov/tao/elnino/nino-home.html

[32]. D.N. Severov, E. Mordecki, and V.A. Pshennikov, SST anomaly variability in Southwestern Atlantic and El Nino/Southern oscillation, Advances in Space Research, Vol. 33, (2004), 343-347.

[33]. http://www.cpc.ncep.noaa.gov/products/analysis_monitoring/ ensostuff/ ensoyears_1877-present.shtml.

Or: http://www.cpc.ncep.noaa.gov/products/analysis_monitoring/ ensostuff/ ensoyears.shtml.

[34]. S. Levitus, J.I. Antonov, J.L. Wang, T.L. Delworth, K.W. Dixon, A.J. Broccoli, Anthropogenic warming of earthps climate system. Science, Vol. 292, (2001), 267.

[35]. http://www.cpc.ncep.noaa.gov/products/precip/CWlink/ MJO/ enso.shtml.

or

http://science.nasa.gov/headlines/y2002/05mar_kelvinwave.htm.

[36]. M. Ausloos and K. Ivanova, Power-law correlations in the southern-oscillation-index fluctuations characterizing El Nino, Physical Review E, Vol. 63, (2001), 047201.

[37]. Richard Metzler, Comment on "power-law correlations in the southern-oscillation-index fluctuations characterizing El Nino", Physical Review E, Vol. 67, (2003), 018201.

[38]. A. RuizdeElvira, and M.J. OrtizBevia, Application of statistical techniques to the analysis and prediction of ENSO: Bayesian oscillation patterns as a prediction scheme, Dynamics of Atmospheres and Oceans, Vol. 22, (1995), 91-114.

[39]. Joel Michaelsen, A statistical study of large-scale, long-period variability in North Pacific sea surface temperature anomalies, Journal of phys-

ical oceanography, Vol. 12, (1982), 694-703.

[40]. V.E. Privalsky, Stochastic models and spectra of interannual variability of mean annual sea surface temperature in the north Atlantic. Dynamics of Atmospheres and Oceans, Vol. 12, (1988), 1-18.

[41]. Klaus Fraedrich, and Richard Blender, Scaling of Atmosphere and Ocean Temperature Correlations in Observatins and Climate Models, Physical Review Letters, Vol. 90, Number 10, (2003), 108501.

[42]. Tomoki Tozuka, Jing-Jia Luo, Sebastien Masson, Swadhin K. Behera, Toshio Yamagata, Annual ENSO simulated in a coupled ocean-atmosphere model, Dynamics of Atmospheres and Oceans, Vol. 39, (2005), 41-60.